

UC San Diego

UC San Diego Previously Published Works

Title

Substrate-Specific Inhibition Constants for Phospholipase A2 Acting on Unique Phospholipid Substrates in Mixed Micelles and Membranes Using Lipidomics

Permalink

<https://escholarship.org/uc/item/0v686469>

Journal

Journal of Medicinal Chemistry, 62(4)

ISSN

0022-2623

Authors

Mouchlis, Varnavas D
Armando, Aaron
Dennis, Edward A

Publication Date

2019-02-28

DOI

10.1021/acs.jmedchem.8b01568

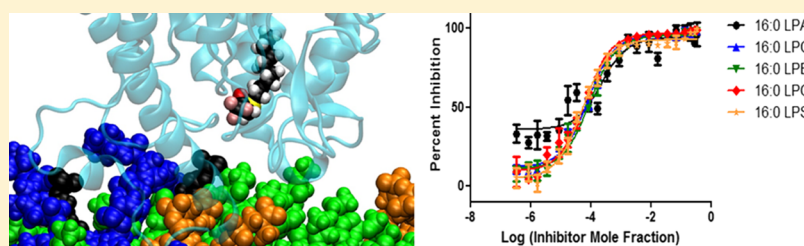
Peer reviewed

Substrate-Specific Inhibition Constants for Phospholipase A₂ Acting on Unique Phospholipid Substrates in Mixed Micelles and Membranes Using Lipidomics

Varnavas D. Mouchlis,*¹ Aaron Armando, and Edward A. Dennis*

Department of Chemistry and Biochemistry and Department of Pharmacology, School of Medicine, University of California, San Diego, La Jolla, California 92093-0601, United States

S Supporting Information



ABSTRACT: Assaying lipolytic enzymes is extremely challenging because they act on water-insoluble lipid substrates, which are normally components of micelles, vesicles, and cellular membranes. We extended a new lipidomics-based liquid chromatographic–mass spectrometric assay for phospholipases A₂ to perform inhibition analysis using a variety of commercially available synthetic and natural phospholipids as substrates. Potent and selective inhibitors of three recombinant human enzymes, including cytosolic, calcium-independent, and secreted phospholipases A₂ were used to establish and validate this assay. This is a novel use of dose–response curves with a mixture of phospholipid substrates, not previously feasible using traditional radioactive assays. The new application of lipidomics to developing assays for lipolytic enzymes revolutionizes in vitro testing for the discovery of potent and selective inhibitors using mixtures of membranelike substrates.

INTRODUCTION

Assaying the activity of phospholipases A₂ (PLA₂s) has been challenging because they are water-soluble enzymes acting on water-insoluble phospholipid substrates.^{1,2} To set up a successful PLA₂ assay, one must consider three critical issues. First, a suitable phospholipid substrate must be used because there is a variety of available phospholipids. Second, phospholipids exist in aggregated forms in water and so the appropriate physical form should be employed. Third, a sensitive detection system must be used that is compatible with the substrate.³ Traditional PLA₂ assays have employed synthetic radio-labeled phospholipids that contain ³H- or ¹⁴C-labeled fatty acids (FAs) at the sn-2 position of the phospholipid. Such phospholipids are challenging to synthesize, expensive, and limited in terms of commercial availability, and they require special handling techniques.⁴ These limitations pose significant difficulties in choosing an optimum substrate for each of the various types of PLA₂s. The surface-dilution kinetics model was successfully employed by our laboratory to explain the action of PLA₂ enzymes on phospholipid/detergent mixed micelles.^{5,6} The success of the surface dilution model to explain kinetics of PLA₂ enzymes in mixed micelles, the stability of the micelle structure in the presence of various phospholipids or inhibitors, and high efficiency in preparing mixed micelles make them a suitable physical form of a substrate to employ in a PLA₂ assay.⁷

Lipidomics-based liquid chromatographic–mass spectrometric (LC–MS) approaches have proven to be very powerful in understanding how PLA₂ enzymes regulate eicosanoid biosynthesis.^{8,9} LC–MS provides a very sensitive detection system that is compatible with mixed micelles in the presence of a surfactant.

A novel lipidomics-based PLA₂ assay using mixed micelles was previously developed for substrate specificity studies on three human enzymes including group IVA cytosolic (cPLA₂), group VIA calcium-independent (iPLA₂), and group V secreted PLA₂ (sPLA₂).¹⁰ This assay is semi-high throughput, uses significantly smaller amounts of substrate and enzyme compared to existing assays,^{3,4} and allows the use of a wide variety of natural and synthetic unlabeled phospholipids. In the current study, we have further developed our assay to obtain inhibitory dose–response curves using a variety of pure phospholipids, not previously feasible using traditional radioactive assays. Three potent and selective inhibitors, one each specific for cPLA₂, iPLA₂, and sPLA₂, were employed to validate the use of the assay for inhibitor studies. The ability to employ lipidomics techniques in assaying PLA₂ enzymes allowed us for the first time to perform more complex inhibitory assessments with mixtures of phospholipids.

Received: October 9, 2018

Published: January 7, 2019

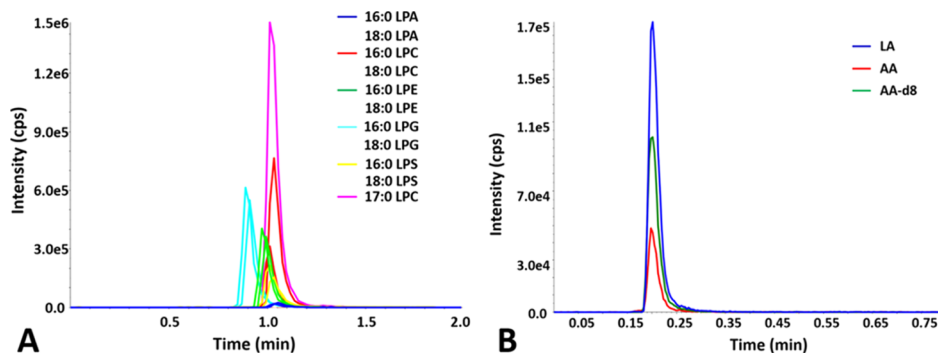


Figure 1. Quantification of primary and internal standards using HPLC chromatography and MRM: (A) for lysophospholipids using a HILIC column (adapted from ref 10) and (B) for free FAs using a C18 reversed-phase column.

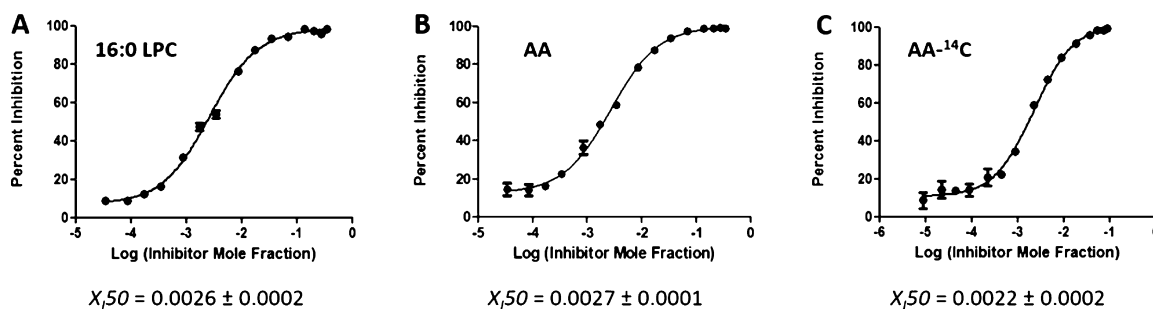


Figure 2. Dose–response inhibition curves for pyrrophenone using PABC substrate. (A) Activity of cPLA₂ was measured by detecting 16:0 LPC in a positive ion mode and (B) by detecting free AA in a negative ion mode. (C) Activity of the enzyme was measured using ¹⁴C-labeled AA in a scintillation counter.

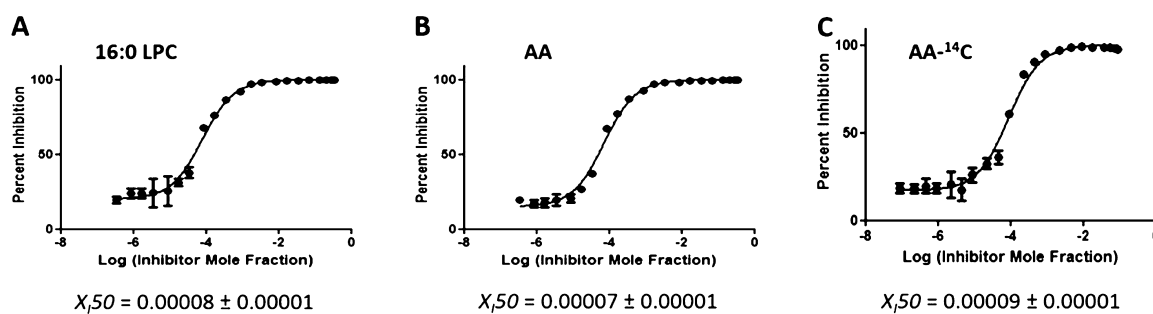


Figure 3. Dose–response inhibition curves for OTFP using PABC substrate. (A) Activity of iPLA₂ was measured by detecting 16:0 LPC in a positive ion mode and (B) by detecting free AA in a negative ion mode. (C) Activity of the enzyme was measured using ¹⁴C-labeled AA in a scintillation counter.

Determining $X_1(50)$ and IC_{50} values using a membranelike substrate is now feasible, which should aid in identifying potent and selective inhibitors for PLA₂ enzymes that are necessary for the development of new therapeutics.

RESULTS AND DISCUSSION

Assay Development and Validation. A lipidomics-based high-performance LC (HPLC)–MS assay using hydrophilic interaction chromatography (HILIC) and multiple reaction monitoring (MRM), which allowed quantification of a variety of lysophospholipid products, was previously developed by us and employed to define the substrate specificity for cPLA₂, iPLA₂, and sPLA₂ (Figure 1A).¹⁰ We have now used and also extended the assay to use C18 reversed-phase chromatography for the quantification of free FA products, including arachidonic acid (AA), deuterated AA (AA-d8), and linoleic acid (LA, Figure 1B). 17:0 LPC and AA-d8 were used as internal standards for normalizing variations related to sample

handling, ionization efficiency, and signal intensity fluctuations. Lysophospholipids and free FAs were detected using the positive and negative ion mode, respectively.¹⁰

Three inhibitors were used to develop and validate the PLA₂ assay: pyrrophenone, which is a pyrrolidine cPLA₂ inhibitor;¹¹ OTFP, which is a fluoroketone iPLA₂ inhibitor;¹² and Ly315920, which is an indole sPLA₂ inhibitor.¹³ For each inhibitor, three dose–response inhibition curves were generated for calculating $X_1(50)$ and IC_{50} values: two by using lipidomics assays (one measuring lysophospholipid product in the positive ion mode and one the FA product in the negative ion mode) and one by using the traditional radioactive assay. $X_1(50)$ is the mole fraction of the inhibitor in the total substrate interface required to inhibit the enzyme by 50%.¹⁴ $X_1(50)$ and IC_{50} values were calculated by plotting the percentage of inhibition versus log (mole fraction) or log (concentration), respectively. For the radioactive assay, a phospholipid substrate containing ¹⁴C-labeled AA esterified at

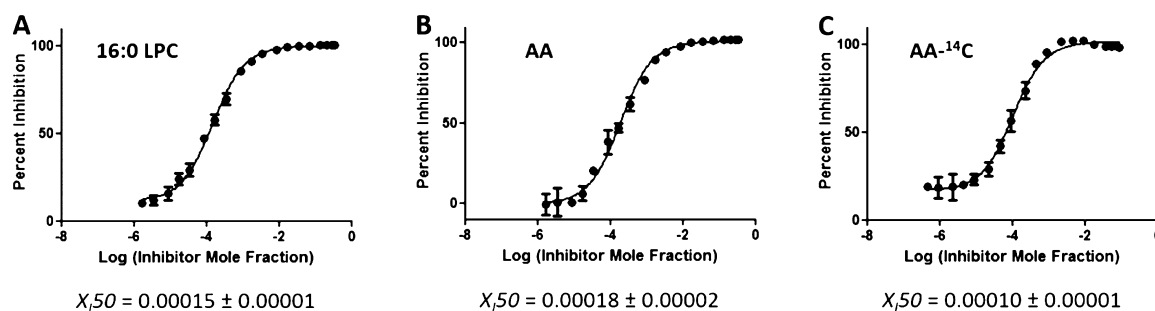
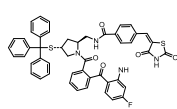
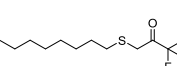
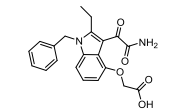


Figure 4. Dose–response inhibition curves for Ly315920 using PAPC substrate. (A) Activity of sPLA₂ was measured by detecting 16:0 LPC in a positive ion mode and (B) by detecting free AA in a negative ion mode. (C) Activity of the enzyme was measured using ¹⁴C-labeled AA in a scintillation counter.

Table 1. $X_{i,50}$ and IC_{50} (μ M) Values of PLA₂ Inhibitors

#	Substrate Inhibitor Structure	PAPA		PAPC		PAPE		PAPG		PAPS		PLPC		
		$X_{i,50}$	IC_{50}	$X_{i,50}$	IC_{50}	$X_{i,50}$	IC_{50}	$X_{i,50}$	IC_{50}	$X_{i,50}$	IC_{50}	$X_{i,50}$	IC_{50}	
1	 Pyrrophenone	Single phospholipid species												
				0.0026 ^a ± 0.0002	1.83 ^a ± 0.14									
				0.0027 ^b ± 0.0001	1.88 ^b ± 0.10									
		0.0022 ^c ± 0.0002	1.23 ^c ± 0.08											
		Equal molar mixture of PAPA, PAPC, PAPE, PAPG, and PAPS												
		0.00013 ^a ± 0.0001	0.09 ^a ± 0.08	0.0020 ^a ± 0.0001	1.39 ^a ± 0.09	0.0022 ^a ± 0.0001	1.52 ^a ± 0.10	0.0026 ^a ± 0.0001	1.82 ^a ± 0.09	0.0020 ^a ± 0.0001	1.41 ^a ± 0.13			
2	 OTFP	Single phospholipid species												
				0.00008 ^a ± 0.00001	0.054 ± 0.005							0.00012 ^a ± 0.00002	0.083 ^a ± 0.011	
				0.00007 ^b ± 0.00001	0.049 ± 0.004							0.00010 ^b ± 0.00001	0.067 ^b ± 0.005	
		0.00009 ^c ± 0.00001	0.048 ± 0.005											
		Equal molar mixture of PAPA, PAPC, PAPE, PAPG, and PAPS												
		0.0002 ^a ± 0.0001	0.16 ^a ± 0.06	0.00008 ^a ± 0.0001	0.054 ^a ± 0.005	0.00009 ^a ± 0.0001	0.063 ^a ± 0.007	0.00006 ^a ± 0.0001	0.048 ^a ± 0.005	0.00005 ^a ± 0.0001	0.046 ^a ± 0.004			
3	 Ly 315920	Single phospholipid species												
				0.00015 ^a ± 0.00001	0.104 ^a ± 0.006				0.026 ^a ± 0.002	18 ^a ± 2				
				0.00018 ^b ± 0.00002	0.131 ^b ± 0.011				0.032 ^b ± 0.002	22 ^b ± 1				
		0.00010 ^c ± 0.00001	0.056 ^c ± 0.005											
		Equal molar mixture of PAPA, PAPC, PAPE, PAPG, and PAPS												
		0.0006 ^a ± 0.0010	0.38 ^a ± 0.72	0.0013 ^a ± 0.0002	0.91 ^a ± 0.11	0.0009 ^a ± 0.0001	0.59 ^a ± 0.08	0.0031 ^a ± 0.0004	2.14 ^a ± 0.25	0.0005 ^a ± 0.0001	0.33 ^a ± 0.04			
						0.0008 ^b ± 0.0001	0.60 ^b ± 0.1							

^aPLA₂ activity was measured by detecting 16:0 lysophospholipid product in a positive ion mode. ^bPLA₂ activity was measured by detecting free AA product in a negative ion mode. ^cPLA₂ activity was measured by using ¹⁴C-labeled AA.

Table 2. $X_{i,50}$, IC_{50} , and Standard Error Values for the Inhibition of cPLA₂ by Pyrrophenone, iPLA₂ by OTFP, and sPLA₂ by Ly315920, Respectively, Calculated by Performing Three Independent Dose–Response Inhibition Experiments on Each Inhibitor

	pyrrophenone				OTFP				LY315920			
	positive		negative		positive		negative		positive		negative	
	$X_{i,50}$	IC_{50} (μ M)	$X_{i,50}$	IC_{50} (μ M)	$X_{i,50}$	IC_{50} (μ M)	$X_{i,50}$	IC_{50} (μ M)	$X_{i,50}$	IC_{50} (μ M)	$X_{i,50}$	IC_{50} (μ M)
	0.0027	1.83	0.0027	1.88	0.00008	0.054	0.00007	0.049	0.00015	0.104	0.00019	0.131
	0.0019	1.32	0.0020	1.38	0.00008	0.058	0.00009	0.060	0.00018	0.124	0.00018	0.127
	0.0023	1.61	0.0021	1.47	0.00007	0.051	0.00005	0.034	0.00017	0.116	0.00020	0.136
average	0.0023	1.59	0.0023	1.58	0.00008	0.055	0.00007	0.048	0.00017	0.114	0.00019	0.131
STDEV	0.0004	0.26	0.0004	0.27	0.000005	0.004	0.00002	0.013	0.00001	0.010	0.00001	0.004

the sn-2 position was used. Free ¹⁴C-labeled AA was detected using a scintillation counter. Mixed micelles were prepared using 1-palmitoyl-2-arachidonoyl-*sn*-glycero-3-phosphocholine (PAPC) and C12E8 surfactant. PAPC was chosen as a

substrate because cPLA₂ is selective for AA at the sn-2 position and to have a common substrate for comparison of our results because iPLA₂ and sPLA₂ exhibit fair activity toward this substrate. Figures 2–4 show the dose–response curves for

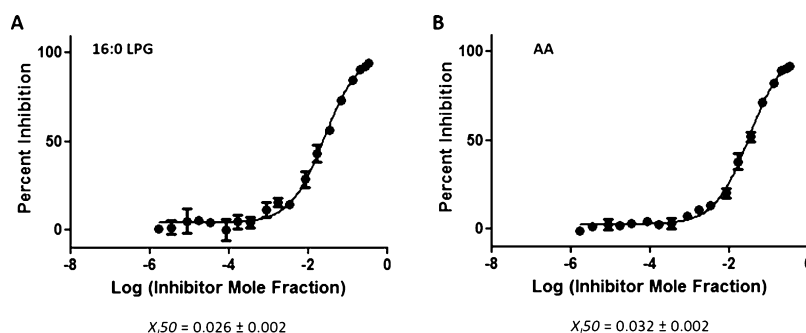


Figure 5. Dose–response inhibition curves for Ly315920 using PAPG substrate. (A) Activity of sPLA₂ was measured by detecting 16:0 LPG in a positive ion mode and (B) by detecting free AA in a negative ion mode.

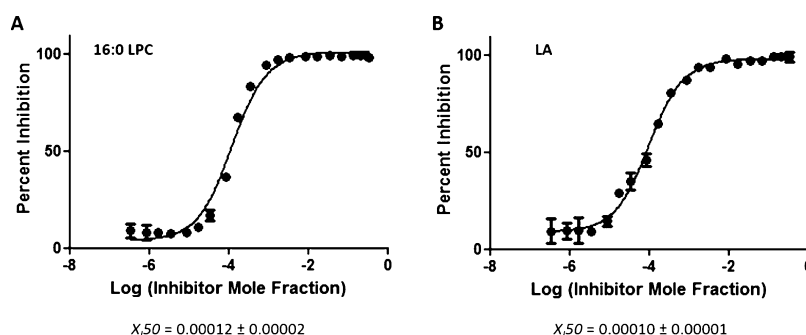


Figure 6. Dose–response inhibition curves of OTFP using PLPC substrate. (A) Activity of iPLA₂ was measured by detecting 16:0 LPC in a positive ion mode and (B) by detecting free LA in a negative ion mode.

pyrrophenone, OTFP, and Ly315920, respectively. $X_1(50)$ values of 0.0026 ($IC_{50} = 1.83 \mu\text{M}$) and 0.0027 ($IC_{50} = 1.88 \mu\text{M}$) were calculated for pyrrophenone using the lipidomics assay in positive and negative ion mode, respectively (Figures 2A,B). An $X_1(50)$ value of 0.0022 ($IC_{50} = 1.23 \mu\text{M}$) was determined for the same inhibitor using the radioactive assay (Figure 2C). The $X_1(50)$ values for OTFP were 0.00008 ($IC_{50} = 0.054 \mu\text{M}$) and 0.00007 ($IC_{50} = 0.049 \mu\text{M}$) using the lipidomics assay (Figure 3A,B) and 0.00009 ($IC_{50} = 0.048 \mu\text{M}$) using the radioactive assay (Figure 3C). Finally, $X_1(50)$ values of 0.00015 ($IC_{50} = 0.104 \mu\text{M}$) and 0.00018 ($IC_{50} = 0.131 \mu\text{M}$) (Figure 4A,B) were determined for Ly315920 using the lipidomics assay and 0.00010 ($IC_{50} = 0.056 \mu\text{M}$) using the radioactive assay (Figure 4C). The $X_1(50)$ and IC_{50} values that were determined using the lipidomics and radioactive assays were very similar for each of the three inhibitors within the calculated experimental error, indicating the validity of the lipidomics assays (Table 1).

To further assess the accuracy of lipidomics assays, three independent dose–response inhibition experiments were performed for each inhibitor (Figures S1–S3). The reported average $X_1(50)$, IC_{50} , and the standard error values indicate the reproducibility, robustness, and accuracy of the lipidomics assay (Table 2).

Substrate Affinity Affects Competitive Inhibitors. The identification of a variety of lysophospholipid and free FA products using LC–MS (Figure 1) enabled us to perform dose–response inhibition curves by using phospholipid substrates with a better affinity toward these enzymes. On the basis of substrate specificity data, sPLA₂ showed approximately 27-fold greater activity toward phospholipids containing phosphoglycerol (PG) compared to PAPC.¹⁰ The dose–response inhibition studies of Ly315920 in the presence

of 1-palmitoyl-2-arachidonoyl-*sn*-glycero-3-phosphoglycerol (PAPG) gave $X_1(50)$ values of 0.026 ($IC_{50} = 18 \mu\text{M}$) and 0.032 ($IC_{50} = 22 \mu\text{M}$) in positive and negative ion modes, respectively (Figure 5A,B). Ly315920 showed approximately a 170-fold higher inhibitory potency toward sPLA₂ when PAPC was utilized as a substrate versus PAPG. iPLA₂ exhibited approximately fourfold higher activity toward phospholipids containing linoleic (L) acid at the *sn*-2 position rather than AA.¹⁰ $X_1(50)$ values of 0.00012 ($IC_{50} = 0.083 \mu\text{M}$) and 0.00010 ($IC_{50} = 0.067 \mu\text{M}$) were determined for OTFP in positive and negative ion modes, respectively, by using PLPC as a substrate (Figure 6A,B). OTFP exhibited approximately twofold greater inhibitor potency toward iPLA₂ when PAPC was used as a substrate versus PLPC. These two examples demonstrate that the inhibitory potency is dependent on the substrate affinity when it comes to competitive inhibitors.

Inhibition Studies on Membranelike Mixtures of Substrates. PLA₂ enzymes are localized on different cellular membranes where they encounter different substrates depending on their cellular localization. Cellular membranes consist of a wide variety of phospholipids that are substrates for PLA₂ enzymes with different affinities. Two factors affect the activity of a PLA₂ enzyme toward a particular phospholipid substrate including the association of the enzyme with the membrane and the specific binding of the phospholipid in the active site. To study the effect of the interfacial association with the membrane on dose–response inhibition studies, a more complex system of an equal molar mixture of five phospholipid species was used to determine $X_1(50)$ values. The *sn*-1 and *sn*-2 positions of each phospholipid contained palmitic (P) and arachidonic (A) acid, respectively, whereas the head groups were varied including phosphatidic acid (PA), phosphocholine (PC), phosphoethanolamine (PE), PG, or phosphoserine

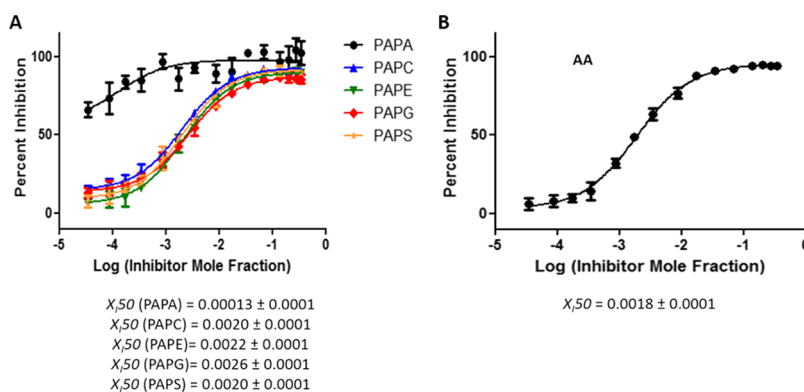


Figure 7. Dose–response inhibition curves for pyrrophenone using an equal molar mixture of 1-palmitoyl-2-arachidonoyl-*sn*-glycero-3-phosphate (PAPA), PAPC, 1-palmitoyl-2-arachidonoyl-*sn*-glycero-3-phosphoethanolamine (PAPE), PAPG, and PAPS as a substrate. (A) Activity of cPLA₂ was measured by detecting 16:0 LPA, 16:0 LPC, 16:0 LPE, 16:0 LPG, and 16:0 LPS in a positive ion mode and (B) by detecting free AA in a negative ion mode.

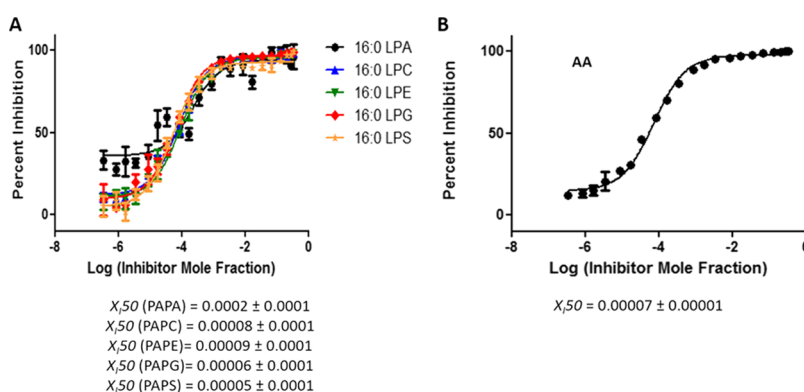


Figure 8. Dose–response inhibition curves for OTFP using an equal molar mixture of PAPA, PAPC, PAPE, PAPG, and PAPS as a substrate. (A) Activity of iPLA₂ was measured by detecting 16:0 LPA, 16:0 LPC, 16:0 LPE, 16:0 LPG, and 16:0 LPS in a positive ion mode and (B) by detecting free AA in a negative ion mode.

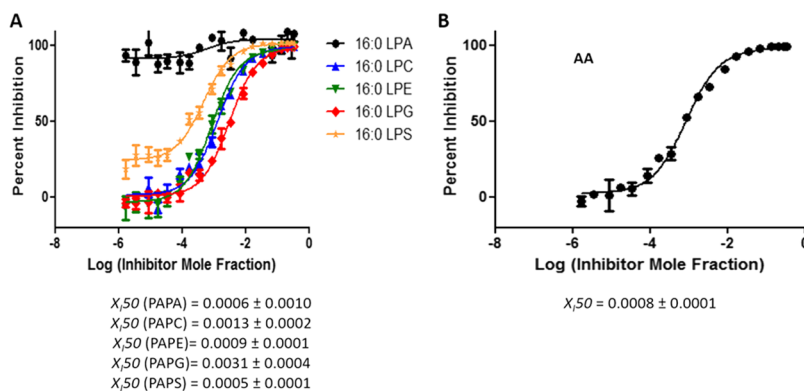


Figure 9. Dose–response inhibition curves for Ly315920 using a mixture of PAPA, PAPC, PAPE, PAPG, and PAPS as a substrate. (A) Activity of sPLA₂ was measured by detecting 16:0 LPA, 16:0 LPC, 16:0 LPE, 16:0 LPG, and 16:0 LPS in a positive ion mode and (B) by detecting free AA in a negative ion mode.

(PS). The $X_{i,50}$ values of pyrrophenone and OTFP, determined in positive ion mode, were similar for each of the five phospholipids individually with some variations because of human and instrumental error (Figures 7A and 8A). $X_{i,50}$ values based on total AA released of 0.0018 (IC_{50} = 1.30 μ M) and 0.00007 (IC_{50} = 0.050 μ M) were determined for pyrrophenone and OTFP, respectively, which do not differ significantly from the ones determined for each phospholipid separately in a positive ion mode (Figures 7B and 8B).

According to the substrate specificity data, cPLA₂ and iPLA₂ did not exhibit significant preference for the sphingolipid headgroup;¹⁰ thus, the $X_{i,50}$ values of pyrrophenone and OTFP were not affected significantly in mixtures. In contrast, as previously reported, sPLA₂ showed strong preference for PAPG compared to the other four phospholipid species.¹⁰ For Ly315920, an $X_{i,50}$ value of 0.0031 (IC_{50} = 2.14 μ M) was determined for PAPG as a substrate which is significantly higher than the $X_{i,50}$ values for the other four phospholipids

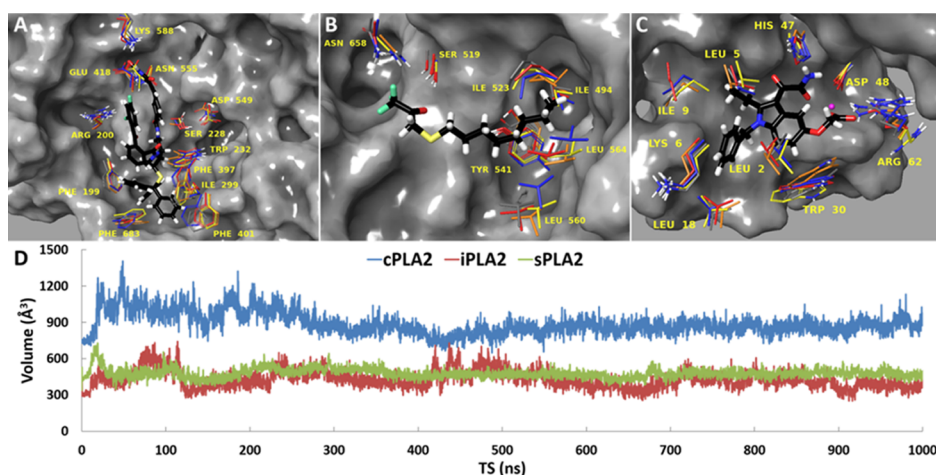


Figure 10. MD simulations and clustering analysis allowed the identification of dynamic structures suitable for in silico screening of compound libraries for (A) cPLA₂, (B) iPLA₂, and (C) sPLA₂. (D) Active site volume during the time of the simulation for cPLA₂, iPLA₂, and sPLA₂ is shown.

(Figure 9A). By detecting AA in a negative ion mode, a total composite $X_1(50)$ value was determined for the phospholipid mixture because this FA is common in all five phospholipids. An $X_1(50)$ value of 0.0008 ($IC_{50} = 0.60 \mu M$) was determined for Ly315920, which differs from the ones determined for each of the five phospholipids using a positive ion mode (Figure 9B). Furthermore, the $X_1(50)$ values for PAPS and PAPA (the least good substrates) are higher than those for PAPE and PAPC, the next best substrates, and lowest for PAPG, the best substrate, in the order expected. This demonstrates that one can enlarge the dynamic range of experimentally determining inhibition constants by judicious choice of substrate and substrate mixtures.

Application of PLA₂ Assay Combined with Molecular Dynamics to Identify Novel Inhibitors. Elucidating the biological function of cPLA₂, iPLA₂, and sPLA₂ is very important because they are involved in several inflammatory diseases including cancer, diabetes, and atherosclerosis.¹ Small organic molecules with potent and selective inhibitory properties are essential tools for studying the biological function of these enzymes. This in vitro assay can be combined with in silico screening techniques to identify new hit compounds for each enzyme. Because the available three-dimensional structures of these enzymes do not contain a bound inhibitor, molecular docking was employed to create an initial enzyme–inhibitor complex that was consistent with previously published HD-XMS data.^{12,15,16} Each complex was then placed on the surface of the membrane based on previous models for each enzyme binding to membranes.¹⁰ In the context of the relaxed complex scheme, which combines the advantages of molecular docking with dynamic structural information,¹⁷ each system was subjected to molecular dynamics (MD) simulations in the presence of a membrane. Movies 1, 2, and 3 show the binding interaction of pyrrophenone, OTFP, and Ly315920 in the active site of cPLA₂, iPLA₂, and sPLA₂, respectively. Clustering analysis allowed the identification of dynamic structures for each enzyme (Figure 10A–C). These structures will be used to virtually screen compound libraries, select a reasonable number of good binders, and test them in vitro using the PLA₂ LC–MS assay described herein. Even though cPLA₂, iPLA₂, and sPLA₂ can bind and hydrolyze the same phospholipid substrate, cPLA₂ binds large inhibitors similar to pyrrophenone, whereas

iPLA₂ and sPLA₂ bind relatively small inhibitors such as OTFP and Ly312059. The volume of the cPLA₂ active site was stabilized at $\sim 900 \text{ \AA}^3$ during the simulation, whereas the volume of the iPLA₂ and sPLA₂ active site was stabilized at $\sim 500 \text{ \AA}^3$ (Figure 10D). This indicates that iPLA₂ and sPLA₂ can adjust the volume of their active site by recruiting small molecule inhibitors that optimize interactions with small binding pockets.

CONCLUSIONS

Assaying PLA₂ enzymes using traditional radioactive assays has been extremely limiting because radiolabeled phospholipid substrates are challenging to synthesize and purify and few are available commercially. In this article, we present a novel lipidomics PLA₂ assay which is simple, semi-high throughput, and does not require the use of radiolabeled phospholipid. The LC–MS-based system described herein has a sensitivity similar to the radioactive assay. The new assay was validated by using pyrrophenone, OTFP, and Ly315920, which are potent inhibitors for cPLA₂, iPLA₂, and sPLA₂, respectively. Because detailed dose–response inhibition studies proved the robustness of the assay, it is now possible to use it with mixtures of phospholipids and in combination with in silico screening to identify novel PLA₂ inhibitors.

In the classic radiolabeled assay, the radiolabeled substrate is used as a tracer for a particular phospholipid which is present (i.e., 1-palmitoyl-2-(1-[¹⁴C]-arachidonoyl)-sn-glycero-3-phosphocholine for PAPC); therefore, if a mixture of phospholipids was included as a substrate, the hydrolysis of the radiolabeled substrate would be competing with other nonlabeled phospholipids as a substrate, so the apparent activity would depend on the specific phospholipid mixture used. In contrast with the lipidomics assay, the specific lysophospholipid and the specific FA products can each be detected for each different phospholipid in the mixture. This is illustrated in Figures 7 and 8 whereby in the presence of an inhibitor, the net activity (expressed as $X_1(50)$ or IC_{50}) reflects the inhibitor binding to the enzyme effecting its affinity for each substrate phospholipid proportionally. For these two enzymes (cPLA₂ and iPLA₂), each of the five substrates in the mixture has a similar affinity for the enzyme; therefore, the $X_1(50)$ or IC_{50} are the same, measured for each lysophospholipid product and for the total AA released from all five phospholipids. In contrast, in Figure 9

with sPLA₂, where the affinity for each phospholipid substrate is different, the X₁(50) or IC₅₀ for the sPLA₂ specific inhibitor is different for each phospholipid. If one of the phospholipids in the mixture was not a substrate for the enzyme as might be the case in a natural membrane, then no lysophospholipid or FA products would appear for that phospholipid, but one could still determine the X₁(50) or IC₅₀ for the inhibition of the enzyme acting on each of the other phospholipids present.

Additionally, it is important to test inhibitors on natural substrates found in the membrane of the specific subcellular organelle that each enzyme acts on. Mixtures of phospholipids with varying sn-2 FA leaving groups and polar groups can now be combined to mimic natural membranes, and the resulting activity of each PLA₂ can be determined. This new approach to assaying PLA₂s will allow us to determine if a given inhibitor is more effective with one substrate over another. We are now exploring the extension of this in vitro assay to determine the ex vivo activity of these enzymes in living cells, where the analysis of the products after enzyme activation in the cells should provide greater insight as to the relevance to the in vivo activity.

■ EXPERIMENTAL AND COMPUTATIONAL METHODS

Lipidomics PLA₂ Assay. Group-specific assays were employed to determine the activity of human recombinant group IVA cytosolic (cPLA₂), group VIA calcium-independent (iPLA₂), and group V secreted PLA₂ (sPLA₂) in a mixed micelle 96 well-plate assay, as previously described.¹⁰ The substrate for each enzyme consisted of 100 μM of phospholipid, 400 μM of C12E8 surfactant, 2.5 μM of 17:0 LPC, and 10 μM AA-d8 internal standards for positive and negative ion modes, respectively. For cPLA₂, the total phospholipid concentration (100 μM) consisted of 97 μM phospholipid substrate and 3 μM PI(4,5)P₂, which enhances the activity of the enzyme. A specific buffer was prepared to achieve optimum activity for each enzyme. The buffer for cPLA₂ contained 100 mM HEPES of pH 7.5, 90 μM CaCl₂, and 2 mM DTT. For iPLA₂, the buffer consisted of 100 mM HEPES of pH 7.5, 2 mM ATP, and 4 mM DTT. Finally, the buffer for sPLA₂ contained 50 mM Tris-HCl of pH 8.0 and 5 mM CaCl₂. The enzymatic reaction was performed in a 96-well plate using a Benchmark Scientific H5000-H MultiTherm heating shaker for 30 min at 40 °C. Each reaction was quenched with 120 μL of methanol/acetonitrile (ACN; 80/20, v/v), and the samples were analyzed using the HPLC–MS system. A blank experiment, which did not contain enzyme, was also included for each substrate to determine the nonenzymatic hydrolysis product and to detect any changes in the intensity of both 17:0 LPC and AA-d8 internal standards. For each inhibitor dose–response curve, three replicates were performed for each inhibitor concentration during three independent experiments. The standard deviation was calculated for each triplicate and is included in each graph with error bars. Each inhibitor was dissolved in dimethyl sulfoxide at a 5 mM concentration. The radioactive assay was extensively described in previous publications.^{12,16} Dose–response inhibition curves were generated using GraphPad Prism 5.0 and the nonlinear regression by plotting percentage of inhibition versus log (mole fraction) or log (concentration) to calculate the reported X₁(50) and IC₅₀ values and their associated error.

High-Performance Liquid Chromatography–Mass Spectrometry/Mass Spectrometry. A Shimadzu HPLC system consisting of a system controller (SCL-10Avp) with two HPLC pumps (LC-10ADvp), a CTC Analytics PAL autosampler platform (Leap Technologies), and a column controller instrument (Analytical Sales & Products, Inc) were employed for the LC analysis. Mass spectrometric analysis was performed using an AB Sciex 4000 QTRAP triple quadrupole/linear ion trap hybrid mass spectrometer equipped with a Turbo V ion source.¹⁰

Chromatography (HPLC). For separation and quantification of the lysophospholipids, a Phenomenex Kinetex 2.6 μm HILIC 100 Å column of 30 × 2.1 mm size was used. The binary gradient consisted of (A) ACN/water (95/5, v/v, pH = 8.0) containing 25 mM AcNH₄ and (B) ACN/water (50/50, v/v, pH = 7.5) containing 25 mM AcNH₄. Gradient elution was carried out for 1.6 min at a flow rate of 0.8 mL/min. Gradient conditions were as follows: 0% B for 0.8 min; 0–100% B for 0.4 min; 100% B for 0.3 min; and 100% B for 0.1 min.¹⁰ For separation and quantification of free FAs, a Phenomenex Kinetex 2.6 μm C18 100 Å column of 30 × 2.1 mm size was used. A mobile phase of ACN/water (80/20, v/v, pH = 8.9) containing 10 mM NH₄HCO₃ was used in an isocratic elution. A 10 μL aliquot of each sample was injected into the column. The column temperature was kept at 40 °C. All samples were maintained at 4 °C throughout the analysis.

Mass Spectrometry. Lysophospholipids (primary and internal standards), phospholipids, and surfactants (C12E8) were detected in a positive electrospray ionization (ESI) mode, whereas free FAs in a negative ESI mode. Molecular species were detected as [M + H]⁺ ions in the positive ion mode and as [M – H][–] ions in the negative ion mode. Curtain gas (CUR), nebulizer gas (GS1), and turbo gas (GS2) were set to 10, 50, and 20 psi, respectively. The electrospray voltage was set to +4.5 or –4.5 kV, and the turbo ion spray source temperature was set to 500 °C. Lysophospholipids were analyzed using scheduled MRM. Declustering potentials and collision energies were optimized for each analyte to achieve optimal mass spectrometric detection. Nitrogen was employed as the collision gas. Data acquisitions were performed using Analyst software. MultiQuant software was used to quantify all metabolites.

Reagents. Pyrrophenone was purchased from Cayman Chemical Company and was stated to be 100% pure based on HPLC and TLC. OTFP was synthesized by Dr. Bruce Hammock's group and was stated to be more than 97% pure based on GC, NMR, and TLC.¹⁸ Ly315920 was purchased from Selleckchem and was stated to be more than 99% pure based on NMR and HPLC. Phospholipids, primary standards, and internal standards were purchased from Avanti Polar Lipids, Inc. Optima LC–MS grade ACN, water (H₂O), and HPLC grade ammonium acetate (AcNH₄) were obtained from Fisher Scientific. HPLC great ammonium bicarbonate (NH₄HCO₃) was obtained from Spectrum Chemical Mfg. Corp. Octaethylene glycol monododecyl ether (C12E8) was obtained from Sigma-Aldrich.

MD Simulations. Enzyme–Inhibitor–Membrane Complexes. Initial complexes of each enzyme with pyrrophenone, OTFP, and Ly315920 were generated using molecular docking.¹⁹ The crystal structure of cPLA₂,²⁰ a previously published homology model of iPLA₂ based on patatin,² and a previously published homology model of GV sPLA₂ based on GIIA sPLA₂ were used for docking.¹⁰ The calculations were performed using a previously published docking protocol.^{12,16} The Membrane Builder implemented in CHARMM-GUI was employed to generate enzyme–inhibitor–membrane models for MD simulations.^{21,22} As previously reported, the membrane patch consisted of POPC, SAPC, POPE, POPA, POPG, POPS, SAPI(4,5)-P₂, and cholesterol. The average ratios of the phospholipids were chosen to be 0.48 for PC, 0.27 for PE, 0.10 for PI(4,5)P₂, 0.06 for PS, and 0.09 for PA and PG. The average cholesterol/phospholipid ratio was chosen to be 0.40. These ratios are the average ratio of the nuclear, mitochondrial, and plasma membranes where cPLA₂, iPLA₂, and sPLA₂ are localized, respectively.^{23–26} Each system was solvated with TIP3P water molecules and neutralized with 150 mM sodium chloride (NaCl) using the Visual MD (VMD) package.²⁷

Equilibration and Production Runs. MD simulations were carried out using NAMD 2.12.²⁸ The following minimization and equilibration protocol was performed, as previously described:¹⁰ a minimization of 80 000 steps was initially performed by applying harmonic constraints on the enzyme–inhibitor–membrane that were gradually turned off using a constraint scaling factor, followed by a second 120 000 steps minimization without constraints. An initial equilibration of 10 000 steps was performed by also applying harmonic constraints on the enzyme–inhibitor–membrane that were gradually turned off using the same constraint scaling factor,

followed by a second 10 000 steps equilibration without constraints. During the equilibration, each system was slowly heated and held to 310 K using temperature reassignment with a reassignment frequency of 500 timesteps (1000 fs) and a reassignment increment of 1 K. The above minimization and equilibration protocol was sufficient to induce an appropriate disorder of a fluidlike bilayer and avoid unnatural atomistic positions and failure of the simulations by atoms moving at very high velocities. Each system was finally subjected to a 1 μ s production run. For each production run, the temperature was maintained at 310 K using the Langevin thermostat with Langevin coupling coefficient of 1/ps.²⁹ The NPT ensemble was employed, and the pressure was kept constant at 1.01325 kPa using the Langevin piston method with the “useGroupPressure”, “useFlexibleCell”, and “useConstantArea” parameters turned on.³⁰ A timestep of 2 fs was used in combination with the SHAKE algorithm to hold the bonds of hydrogen atoms similarly constrained.³¹ Nonbonded interactions and full electrostatics were calculated for every 1 and 2 timesteps, respectively. Switching functions are used to smoothly take electrostatic and van der Waals interactions to zero with a switching distance of 10 Å and a cutoff of 12 Å. Long-range electrostatic forces in the periodic system were evaluated using the particle mesh Ewald Sum method with a grid spacing of 1/Å.³² The CHARMM General Force Field (CGenFF) and the CHARMM36 all-atom additive force field and parameters were used for other simulations.^{33,34}

Binding Pocket Volume Calculations. The POVME algorithm was employed for calculating the volume of the binding pocket of each enzyme over the time of each simulation.^{10,35} A total number of 6252 frames from each simulation trajectory was used for the calculations. The frames were aligned on the initial complex that was used to carry out the simulation using VMD and were saved in a multiframe PDB format. To define the “inclusion sphere” that entirely encloses the binding pocket of each enzyme, the center of mass of the residues within 5 Å around the bound inhibitor was used as the *x*, *y*, and *z* coordinates of the sphere. An “inclusion sphere” radius of 11 Å was used. Equidistant points were generated in POVME using a grid spacing of 1 Å and a distance cutoff of 1.09 Å.

■ ASSOCIATED CONTENT

📄 Supporting Information

The Supporting Information is available free of charge on the ACS Publications website at DOI: 10.1021/acs.jmedchem.8b01568.

Atomic coordinates of Pyrrophenone with the catalytic domain of cPLA₂ (PDB)

Atomic coordinates of OTFP with the catalytic domain of iPLA₂ (PDB)

Atomic coordinates of Ly315920 with sPLA₂ (PDB)

Dose–response inhibition curves for pyrrophenone, OTFP, and Ly315920 using PAPC substrate (PDF)

Interactions of Pyrrophenone with the active site of cPLA₂ (MPG)

Interactions of OTFP with the active site of iPLA₂ (MPG)

Interactions of Ly315920 with the active site of sPLA₂ (MPG)

■ AUTHOR INFORMATION

Corresponding Authors

*E-mail: vmouchlis@gmail.com (V.D.M.).

*E-mail: edennis@ucsd.edu. Phone: +1 858 534 3055 (E.A.D.).

ORCID

Varnavas D. Mouchlis: 0000-0002-4235-1867

Notes

The authors declare no competing financial interest.

■ ACKNOWLEDGMENTS

This work was supported by the NIH grant GM20501-42 (E.A.D.). We wish to thank Prof. J. Andrew McCammon for providing the computational power needed for MD simulations. We would also like to thank Carol T. Mu, Deion Sugianto, and Renee Hammons for helping with the analysis, figures, and editing.

■ ABBREVIATIONS

PLA₂, phospholipase A₂; LC–MS, liquid chromatography–mass spectrometry; cPLA₂, group IVA cytosolic phospholipase A₂; iPLA₂, group VIA calcium-independent phospholipase A₂; sPLA₂, group V secreted phospholipase A₂; X₁(50), mole fraction of the inhibitor that is required for 50% inhibition of the enzyme; IC₅₀, concentration of the inhibitor that is required for 50% inhibition of the enzyme; HILIC, hydrophilic interaction chromatography; MRM, multiple reaction monitoring; AA, arachidonic acid; AA-d8, deuterated arachidonic acid; LA, linoleic acid; 170 LPC, 1-heptadecanoyl-*sn*-glycero-3-phosphocholine; PAPC, 1-palmitoyl-2-arachidonoyl-*sn*-glycero-3-phosphocholine; C12E8, octaethylene glycol monododecyl ether; 16:0 LPC, 1-palmitoyl-*sn*-glycero-3-phosphocholine; PG, phosphoglycerol; PAPG, 1-palmitoyl-2-arachidonoyl-*sn*-glycero-3-phosphoglycerol; 16:0 LPG, 1-palmitoyl-*sn*-glycero-3-phosphoglycerol; L, linoleic; PLPC, 1-palmitoyl-2-linoleoyl-*sn*-glycero-3-phosphocholine; P, palmitic; A, arachidonic; PA, phosphatidic acid; PC, phosphocholine; PE, phosphoethanolamine; PS, phosphoserine; 16:0 LPA, 1-palmitoyl-*sn*-glycero-3-phosphate; 16:0 LPE, 1-palmitoyl-*sn*-glycero-3-phosphoethanolamine; 16:0 LPS, 1-palmitoyl-*sn*-glycero-3-phosphoserine; PAPA, 1-palmitoyl-2-arachidonoyl-*sn*-glycero-3-phosphate; PAPE, 1-palmitoyl-2-arachidonoyl-*sn*-glycero-3-phosphoethanolamine; PAPS, 1-palmitoyl-2-arachidonoyl-*sn*-glycero-3-phosphoserine; MD, molecular dynamics

■ REFERENCES

- (1) Dennis, E. A.; Cao, J.; Hsu, Y.-H.; Magrioti, V.; Kokotos, G. Phospholipase A2 Enzymes: Physical Structure, Biological Function, Disease Implication, Chemical Inhibition, and Therapeutic Intervention. *Chem. Rev.* **2011**, *111*, 6130–6185.
- (2) Mouchlis, V. D.; Bucher, D.; McCammon, J. A.; Dennis, E. A. Membranes serve as allosteric activators of phospholipase A₂, enabling it to extract, bind, and hydrolyze phospholipid substrates. *Proc. Natl. Acad. Sci. U.S.A.* **2015**, *112*, E516–E525.
- (3) Reynolds, L. J.; Washburn, W. N.; Deems, R. A.; Dennis, E. A. [1] Assay strategies and methods for phospholipases. *Methods Enzymol.* **1991**, *197*, 3–23.
- (4) Yang, H.-C.; Mosior, M.; Johnson, C. A.; Chen, Y.; Dennis, E. A. Group-Specific Assays That Distinguish between the Four Major Types of Mammalian Phospholipase A₂. *Anal. Biochem.* **1999**, *269*, 278–288.
- (5) Carman, G. M.; Deems, R. A.; Dennis, E. A. Lipid signaling enzymes and surface dilution kinetics. *J. Biol. Chem.* **1995**, *270*, 18711–18714.
- (6) Roberts, M. F.; Deems, R. A.; Dennis, E. A. Dual role of interfacial phospholipid in phospholipase A₂ catalysis. *Proc. Natl. Acad. Sci. U.S.A.* **1977**, *74*, 1950–1954.
- (7) Ribeiro, A. A.; Dennis, E. A. Pmr relaxation times of micelles of the nonionic surfactant triton x-100 and mixed micelles with phospholipids. *Chem. Phys. Lipids* **1975**, *14*, 193–199.
- (8) Norris, P. C.; Gosselin, D.; Reichart, D.; Glass, C. K.; Dennis, E. A. Phospholipase A₂ regulates eicosanoid class switching during inflammasome activation. *Proc. Natl. Acad. Sci. U.S.A.* **2014**, *111*, 12746–12751.

- (9) Dennis, E. A.; Norris, P. C. Eicosanoid storm in infection and inflammation. *Nat. Rev. Immunol.* **2015**, *15*, 511–523.
- (10) Mouchlis, V. D.; Chen, Y.; McCammon, J. A.; Dennis, E. A. Membrane allostery and unique hydrophobic sites promote enzyme substrate specificity. *J. Am. Chem. Soc.* **2018**, *140*, 3285–3291.
- (11) Seno, K.; Okuno, T.; Nishi, K.; Murakami, Y.; Yamada, K.; Nakamoto, S.; Ono, T. Pyrrolidine inhibitors of human cytosolic phospholipase A₂. Part 2. *Bioorg. Med. Chem. Lett.* **2001**, *11*, 587–590.
- (12) Mouchlis, V. D.; Morisseau, C.; Hammock, B. D.; Li, S.; McCammon, J. A.; Dennis, E. A. Computer-aided drug design guided by hydrogen/deuterium exchange mass spectrometry: A powerful combination for the development of potent and selective inhibitors of Group VIA calcium-independent phospholipase A₂. *Bioorg. Med. Chem.* **2016**, *24*, 4801–4811.
- (13) Snyder, D. W.; Bach, N. J.; Dillard, R. D.; Draheim, S. E.; Carlson, D. G.; Fox, N.; Roehm, N. W.; Armstrong, C. T.; Chang, C. H.; Hartley, L. W. Pharmacology of ly315920/s-5920,[[3-(amino-oxoacetyl)-2-ethyl-1-(phenylmethyl)-1h-indol-4-yl] oxy] acetate, a potent and selective secretory phospholipase a₂ inhibitor: A new class of anti-inflammatory drugs, spi. *J. Pharmacol. Exp. Ther.* **1999**, *288*, 1117–1124.
- (14) Kokotos, G.; Six, D. A.; Loukas, V.; Smith, T.; Constantinou-Kokotou, V.; Hadjipavlou-Litina, D.; Kotsovolou, S.; Chiou, A.; Beltzner, C. C.; Dennis, E. A. Inhibition of Group IVA Cytosolic Phospholipase A₂ by Novel 2-Oxoamides in Vitro, in Cells, and in Vivo. *J. Med. Chem.* **2004**, *47*, 3615–3628.
- (15) Burke, J. E.; Babakhani, A.; Gofe, A. A.; Kokotos, G.; Li, S.; Woods, V. L.; McCammon, J. A.; Dennis, E. A. Location of Inhibitors Bound to Group IVA Phospholipase A₂ Determined by Molecular Dynamics and Deuterium Exchange Mass Spectrometry. *J. Am. Chem. Soc.* **2009**, *131*, 8083–8091.
- (16) Mouchlis, V. D.; Limnios, D.; Kokotou, M. G.; Barbayianni, E.; Kokotos, G.; McCammon, J. A.; Dennis, E. A. Development of Potent and Selective Inhibitors for Group VIA Calcium-Independent Phospholipase A₂ Guided by Molecular Dynamics and Structure–Activity Relationships. *J. Med. Chem.* **2016**, *59*, 4403–4414.
- (17) Amaro, R. E.; Baron, R.; McCammon, J. A. An improved relaxed complex scheme for receptor flexibility in computer-aided drug design. *J. Comput.-Aided Mol. Des.* **2008**, *22*, 693–705.
- (18) Wheelock, C. E.; Severson, T. F.; Hammock, B. D. Synthesis of new carboxylesterase inhibitors and evaluation of potency and water solubility. *Chem. Res. Toxicol.* **2001**, *14*, 1563–1572.
- (19) Friesner, R. A.; Murphy, R. B.; Repasky, M. P.; Frye, L. L.; Greenwood, J. R.; Halgren, T. A.; Sanschagrin, P. C.; Mainz, D. T. Extra Precision Glide: Docking and Scoring Incorporating a Model of Hydrophobic Enclosure for Protein–Ligand Complexes. *J. Med. Chem.* **2006**, *49*, 6177–6196.
- (20) Dessen, A.; Tang, J.; Schmidt, H.; Stahl, M.; Clark, J. D.; Seehra, J.; Somers, W. S. Crystal structure of human cytosolic phospholipase a₂ reveals a novel topology and catalytic mechanism. *Cell* **1999**, *97*, 349–360.
- (21) Wu, E. L.; Cheng, X.; Jo, S.; Rui, H.; Song, K. C.; Dávila-Contreras, E. M.; Qi, Y.; Lee, J.; Monje-Galvan, V.; Venable, R. M.; Klauda, J. B.; Im, W. CHARMM-GUI Membrane Buildertoward realistic biological membrane simulations. *J. Comput. Chem.* **2014**, *35*, 1997–2004.
- (22) Lee, J.; Cheng, X.; Swails, J. M.; Yeom, M. S.; Eastman, P. K.; Lemkul, J. A.; Wei, S.; Buckner, J.; Jeong, J. C.; Qi, Y.; Jo, S.; Pande, V. S.; Case, D. A.; Brooks, C. L., 3rd; MacKerell, A. D., Jr.; Klauda, J. B.; Im, W. Charmm-gui input generator for namd, gromacs, amber, openmm, and charmm/openmm simulations using the charmm36 additive force field. *J. Chem. Theory Comput.* **2016**, *12*, 405–413.
- (23) van Meer, G.; Voelker, D. R.; Feigenson, G. W. Membrane lipids: Where they are and how they behave. *Nat. Rev. Mol. Cell Biol.* **2008**, *9*, 112–124.
- (24) Shirai, Y.; Balsinde, J.; Dennis, E. A. Localization and functional interrelationships among cytosolic group iv, secreted group v, and ca²⁺-independent group vi phospholipase a₂s in p388d 1 macrophages using gfp/rfp constructs. *Biochim. Biophys. Acta* **2005**, *1735*, 119–129.
- (25) Song, H.; Bao, S.; Lei, X.; Jin, C.; Zhang, S.; Turk, J.; Ramanadham, S. Evidence for proteolytic processing and stimulated organelle redistribution of iPLA₂β. *Biochim. Biophys. Acta* **2010**, *1801*, 547–558.
- (26) Williams, S. D.; Gottlieb, R. A. Inhibition of mitochondrial calcium-independent phospholipase a₂ (ipla₂) attenuates mitochondrial phospholipid loss and is cardioprotective. *Biochem. J.* **2002**, *362*, 23–32.
- (27) Humphrey, W.; Dalke, A.; Schulten, K. Vmd: Visual molecular dynamics. *J. Mol. Graphics* **1996**, *14*, 33–38.
- (28) Phillips, J. C.; Braun, R.; Wang, W.; Gumbart, J.; Tajkhorshid, E.; Villa, E.; Chipot, C.; Skeel, R. D.; Kalé, L.; Schulten, K. Scalable molecular dynamics with namd. *J. Comput. Chem.* **2005**, *26*, 1781–1802.
- (29) Adelman, S. A. Generalized langevin equation approach for atom/solid-surface scattering: General formulation for classical scattering off harmonic solids. *J. Chem. Phys.* **1976**, *64*, 2375–2388.
- (30) Feller, S. E.; Zhang, Y.; Pastor, R. W.; Brooks, B. R. Constant pressure molecular dynamics simulation: The langevin piston method. *J. Chem. Phys.* **1995**, *103*, 4613–4621.
- (31) Ryckaert, J.-P.; Ciccotti, G.; Berendsen, H. J. C. Numerical integration of the cartesian equations of motion of a system with constraints: Molecular dynamics of n-alkanes. *J. Comput. Phys.* **1977**, *23*, 327–341.
- (32) Essmann, U.; Perera, L.; Berkowitz, M. L.; Darden, T.; Lee, H.; Pedersen, L. G. A smooth particle mesh ewald method. *J. Chem. Phys.* **1995**, *103*, 8577–8593.
- (33) Vanommeslaeghe, K.; Hatcher, E.; Acharya, C.; Kundu, S.; Zhong, S.; Shim, J.; Darian, E.; Guvench, O.; Lopes, P.; Vorobyov, I.; Mackerell, A. C. Charmm general force field: A force field for drug-like molecules compatible with the charmm all-atom additive biological force fields. *J. Comput. Chem.* **2009**, *31*, 671–690.
- (34) Klauda, J. B.; Venable, R. M.; Freites, J. A.; O'Connor, J. W.; Tobias, D. J.; Mondragon-Ramirez, C.; Vorobyov, I.; MacKerell, A. D.; Pastor, R. W. Update of the charmm all-atom additive force field for lipids: Validation on six lipid types. *J. Phys. Chem. B* **2010**, *114*, 7830–7843.
- (35) Durrant, J. D.; de Oliveira, C. A. F.; McCammon, J. A. Povme: An algorithm for measuring binding-pocket volumes. *J. Mol. Graphics Modell.* **2011**, *29*, 773–776.

NOTE ADDED AFTER ASAP PUBLICATION

This paper was published February 4, 2019 without all Supporting Information files included. They have been added and the paper re-posted on February 11, 2019.